fermentation

MDPI

Article

Modeling of Hydrogen Production by Applying Biomass Gasification: Artificial Neural Network Modeling Approach

Sahar Safarian [1,*], Seyed Mohammad Ebrahimi Saryazdi [2], Runar Unnthorsson [1] and Christiaan Richter [1]

[1] Department of Industrial Engineering, Mechanical Engineering and Computer Science, University of Iceland, Hjardarhagi 6, 107 Reykjavik, Iceland; runson@hi.is (R.U.); cpr@hi.is (C.R.)
[2] Department of Energy Systems Engineering, Sharif University of Technologies, Tehran P.O. Box 14597-77611, Iran; ebrahimi@energy.sharif.ir
* Correspondence: sas79@hi.is

Abstract: In order to accurately anticipate the proficiency of downdraft biomass gasification linked with a water–gas shift unit to produce biohydrogen, a model based on an artificial neural network (ANN) approach is established to estimate the specific mass flow rate of the biohydrogen output of the plant based on different types of biomasses and diverse operating parameters. The factors considered as inputs to the models are elemental and proximate analysis compositions as well as the operating parameters. The model structure includes one layer for input, a hidden layer and output layer. One thousand eight hundred samples derived from the simulation of 50 various feedstocks in different operating situations were utilized to train the developed ANN model. The established ANN in the case of product biohydrogen presents satisfactory agreement with input data: absolute fraction of variance (R^2) is more than 0.999 and root mean square error (RMSE) is lower than 0.25. In addition, the relative impact of biomass properties and operating parameters on output are studied. At the end, to have a comprehensive evaluation, variations of the inputs regarding hydrogen-content are compared and evaluated together. The results show that almost all of the inputs show a significant impact on the $sm_{hydrogen}$ output. Significantly, gasifier temperature, SBR, moisture content and hydrogen have the highest impacts on the $sm_{hydrogen}$ with contributions of 19.96, 17.18, 15.3 and 10.48%, respectively. In addition, other variables in feed properties, like C, O, S and N present a range of 1.28–8.6% and proximate components like VM, FC and A present a range of 3.14–7.67% of impact on $sm_{hydrogen}$.

Keywords: biomass gasification; artificial neural network; hydrogen production; downdraft; simulation

Citation: Safarian, S.; Ebrahimi Saryazdi, S.M.; Unnthorsson, R.; Richter, C. Modeling of Hydrogen Production by Applying Biomass Gasification: Artificial Neural Network Modeling Approach. *Fermentation* **2021**, *7*, 71. https://doi.org/10.3390/fermentation7020071

Academic Editor: Thaddeus Ezeji

Received: 13 April 2021
Accepted: 30 April 2021
Published: 1 May 2021

Publisher's Note: MDPI stays neutral with regard to jurisdictional claims in published maps and institutional affiliations.

Copyright: © 2021 by the authors. Licensee MDPI, Basel, Switzerland. This article is an open access article distributed under the terms and conditions of the Creative Commons Attribution (CC BY) license (http://creativecommons.org/licenses/by/4.0/).

1. Introduction

To overcome challenges regarding increasing carbon concentration and climate change, renewable energies like biomass, solar radiations and wind have been encouraged to be used because they do not emit greenhouse gases such as carbon dioxide, which plays an important function in global warming [1–4]. Recently, the interest in biofuels/biomass has grown because of the extensive consideration of sustainable sources of energy [5–7]. Biomass has many advantages over fossil fuels as it is a widely available source of energy, less expensive than fossil fuels and helps prevent climate change by reducing GHG [8–11].

In order to convert biomass to product gas, several thermochemical conversion technologies can be employed. The procedures relying on thermochemical conversion can be classified as liquefaction, pyrolysis, combustion and gasification [12,13] and, amongst them, biomass gasification has been proved as a promising green technology toward conversion of different feedstocks to various energy products [8–10]. Through this complex

system, lignocellulosic materials are transformed to a more valuable gas, investigated as syngas by series reactions at high temperatures [14–16].

The gasification process includes different steps of drying the wet feedstocks, pyrolysis of the dried feedstocks and a reaction part including oxidation, reduction and cracking [13,17]. The product gas of biomass gasification comprises mainly carbon monoxide, hydrogen, carbon dioxide and methane that can be consumed for the production of thermal heat, power or hydrogen [18–20]. Hydrogen occupies the top position among all hydrocarbon fuels from an energy density viewpoint, which is about 122 kJ/kg [21], and it can be utilized as a clean source for fuel cells, heat production and transportation [22–24]. Several technologies were developed to produce hydrogen, like biological operations, biowaste gasification, conventional methane steam reforming, pyrolysis, electrolysis and thermochemical methods of water splitting [14,25].

Biomass gasification, as an attractive technology for the conversion of various types of biowastes to energy, is known to be a sustainable procedure to produce hydrogen [26,27]. Gasification of biowastes has been investigated in several research works from the viewpoint of performance analysis [4,11,28–36]. Nevertheless, just a few works on performance analysis of linked gasification–hydrogen production have been reported [19,37,38]. In order to have a comprehensive analysis of a hydrogen production system via water–gas shift reactors, different modeling approaches based on thermodynamic equilibrium, kinetics, computational fluid dynamics (CFD) and artificial neural networks (ANNs) can be developed. The models derived by equilibrium approaches are independent of the gasifier structure, so can be applied for ideal systems and typical thermodynamic characteristics. However, for a widely complex process, accurate kinetic parameters are needed that are used in kinetic modeling. In calculations relying on CFD, a series of equations of energy, momentum, mass and species through a specific area of the gasifier are solved simultaneously and can then predict the distribution of temperature and concentration. The methods based on ANNs require a huge amount of data and then use a set of mathematical regressions for correlations among input and output data [13,15,39–43]. This method has recently gained interest since it can estimate nonlinear functions without the requirement of the mathematical description of phenomena over the system. Therefore, ANN models are attractive for outcome prediction, while critical interactions of complicated nonlinearities are in a data set, such as for biomass conversion [44–47]. However, very few works have been reported about modeling of biomass gasification by using an ANN method and there is nothing in the field of downdraft gasifiers linked with water–gas shift reactors for hydrogen production.

Therefore, as the main objective in this work, a simulation model derived by an equilibrium approach for biomass gasification connected to a hydrogen plant is developed by applying Aspen Plus. In the next step, an ANN model coming from the simulation results for the considered gasification system, relying on features and output matrixes, is established. In fact, the research aim is to develop an ANN model linked with an equilibrium for the estimation of the specific mass flow rate of hydrogen production ($sm_{hydrogen}$) from 50 different feedstocks in different operating conditions. Then, an attempt is made to investigate the relative impact of biomass properties and operating parameters on $sm_{hydrogen}$. At the end, to have a comprehensive analysis, variations of the inputs on $sm_{hydrogen}$ regarding hydrogen content are compared and analyzed together.

2. Material and Methods

2.1. Method of Simulation

In this part, a simulation model based on an equilibrium approach is established for biomass gasification linked with a water–gas (W–G) shift unit and separation unit for hydrogen production by employing Aspen Plus version 10. In order to compute the physical properties of the normal materials in the gasification process, the equation of state of Peng–Robinson with Boston–Mathias alpha function (PR–BM) was used. The existent models of HCOALGEN and DCOALIGT were also applied for enthalpy and density of biomass and ash that are non-conventional materials. Moreover, the stream of MCINCPSD, including substreams of MIXED, CIPSD and NCPSD classes, was taken into account to describe the structures of biomass and ash that are not available in Aspen Plus materials [20,30,48,49]. The scheme of the simulated system by Aspen Plus is presented in Figure 1.

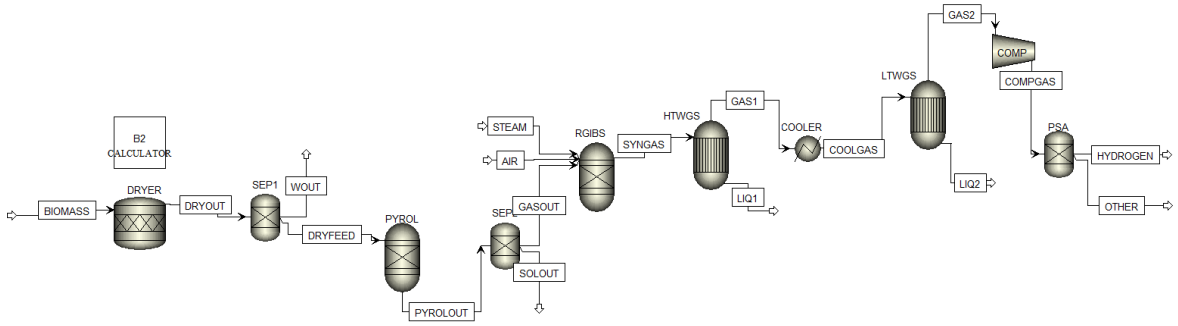

Figure 1. Scheme of the simulated system by Aspen Plus.

2.1.1. Gasification Module

The stream of BIOMASS has been considered as a nonconventional component and it has been defined by the elemental and proximate analyses (E&PAs) of feedstocks. In order to have a detailed work, 50 different biomasses from groups of wood and woody biomasses, and herbaceous and agricultural biomasses, were considered [50]. The E&PAs of these feedstocks are gathered in Table 1 [50–79]. The drying process occurred at 150 °C to attain a moisture content less than 5 wt.% of the original sample. This part was done by RSTOIC which is a stoichiometric reactor in Aspen Plus. This module was utilized to accomplish chemical reactions of recognized stoichiometry [32]. After the drying step, RYIELD as a yield reactor in Aspen Plus was simulated to perform the biomass pyrolysis. In this part, the feed was transformed into volatile materials (VMs) and char. VMs include mainly carbon, hydrogen, oxygen and nitrogen. Moreover, char was changed to ash and carbon, by determining the product distribution based on the E&PAs of the feedstocks. After the pyrolysis process, RGibbs was applied for simulation of the gasification. The pyrolyzed biomass and air or air–steam as a gasifying agent came together in the RGibbs reactor, where partial oxidation and gasification reactions arose. The gasifier reactor estimated the composition of output syngas by minimizing the Gibbs free energy based on the complete chemical equilibrium [80].

Table 1. The range of input and output variables in the ANN model.

Inputs to ANN	**Range**
Moisture (%)	4.4–62.9
Volatile Components (%)	62.3–86.3
Fixed Carbon (%)	12.3–26.3
Ash (%)	0.1–20.1
C (%)	40.03–55.8
O (%)	30.65–44.01
H (%)	4.55–9.7
N (%)	0.096–2.65
S (%)	0–0.446
Gasifier Temperature (°C)	600–1500
Air to Fuel Ratio (kg/kg)	1.8–2.3
Steam to Biomass Ratio (kg/kg)	0.1–0.9
Output Variable for the ANN	**Range**
Specific Mass Flow Rate of Hydrogen (g/kg)	17.25–119.13

2.1.2. Water–Gas Shift Module

For this part, two water–gas shift reactors were considered because the reaction of the W–G shift is relatively exothermic (Equation (1)).

$$CO + H_2O \leftrightarrow CO_2 + H_2 \quad (1)$$

Hence, it needed to have one reactor at higher temperatures (HTWGS) and the other one at lower temperatures (LTWGS). In fact, this reaction went toward the left side at high temperatures. In the HTWGS reactor, firstly, a slight conversion of *CO* with quick kinetics occurred. However, it was not possible to move beyond the equilibrium curve. Therefore, the LTWGS reactor was employed so, by decreasing the operation temperature, it was able to gain higher conversion [81]. HTWGS and LTWGS were simulated at 400 °C and 200 °C with two Requil reactors, respectively [19]. Requil is an equilibrium reactor in which the chemical and phase equilibrium are specified by stoichiometric approaches.

2.1.3. Separation Unit Module

To attain a high purity of hydrogen, a pressure swing adsorption (PSA) unit was applied [82,83]. From the optimal values studied in the literature, the separation efficiency for hydrogen and the input pressure of PSA were considered 70% and 7 bar, respectively [84–87]. Increasing pressure was also carried out by a compressor before the PSA (COMP in Figure 1) and the outlet stream from PSA, defined as HYDROGEN in Figure 1.

As above, 50 biomass feedstocks derived from various groups of woody, herbaceous and agricultural biomasses were entered into the gasification technology as input feedstock. The assessment relied on 1 ton of input feed as a functional unit under atmospheric pressure. The input variables for the developed ANN model were the proximate analysis of biomass containing moisture content, volatile materials, fixed carbon and ash, and the elemental analysis of biomass containing carbon, oxygen, hydrogen, nitrogen and sulfur, along with operating parameters like gasifier temperature, air to fuel ratio and steam to biomass ratio. Table 1 shows the range of input and output variables resulting from the simulation model. It is important to mention that the specific mass flow rate of biohydrogen ($sm_{hydrogen} = \frac{m_{hydrogen}(kg)}{m_{biomass}(kg)}$) is the output result from the simulation model.

2.2. Concept of the Developed ANN Model

In order to investigate the system performance in hydrogen production from the gasification plant, a computational model based on an ANN approach for the considered system was established. The developed ANN comprised a large number of neurons formed in several layers. Neurons of one layer were joined to other neurons in another layer by using weights in order to fulfill a specific task by accurately adjusting the joint weights [88]. The developed ANN model in this work was arranged in the MATLAB® environment by means of the Neural Network Toolbox (nntool). The structure of the ANN model made for the output of $sm_{hydrogen}(kg/kg)$ is shown in Figure 2. For each ANN, one layer was considered for the input layer, hidden layer and output layer. The input layer consisted of 12 variables of M, VM, FC, ash, C, O, H, N and S with units of weight percent (wt.%), gasifier temperature, T (°C), air to fuel ratio ($kg_{air}/kg_{drybiomass}$) and steam to biomass ratio ($kg_{steam}/kg_{drybiomass}$). Actually, there is not a clear method in literature for specifying the number of hidden layers as well as the number of neurons. Therefore, the trial and error method was applied to discover the prime value by means of minimization of the root mean square error (RMSE). The foremost solution was one hidden layer with 13 neurons with intensity of the hydrogen product. Table 2 provides the RMSE values of several ANN structures with different numbers of neurons in the hidden layer. It is indicted that the RMSE decreases by increasing the number of hidden layers from 5 to 13, then it increases moderately when applying more than 13 neurons in the hidden layer because of over-fitting problems.

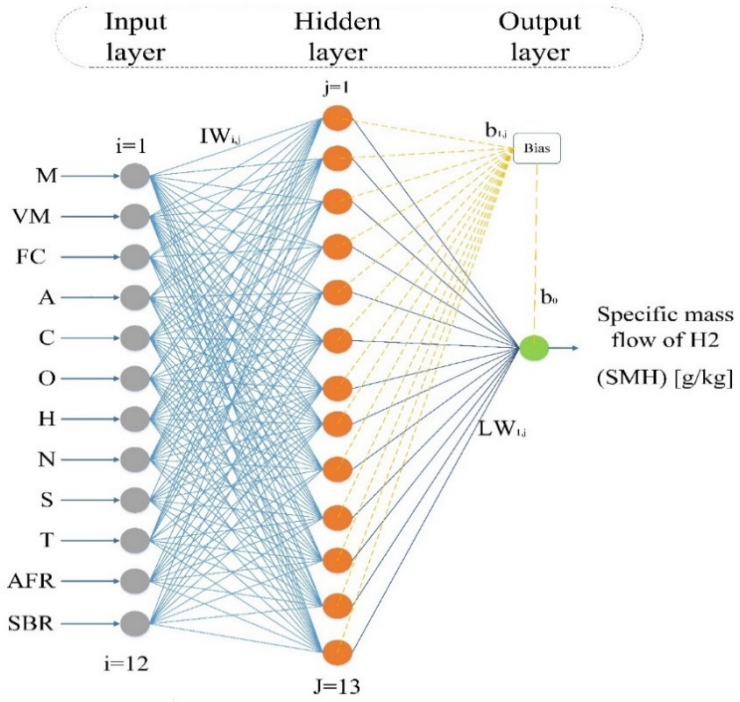

Figure 2. Structure of ANN for prediction of $sm_{hydrogen}(g/kg)$.

Table 2. RMSE values for various ANNs with different structures.

Number of Neurons in Hidden Layer	RMSE
5	0.711
7	0.534
11	0.307
13	0.246
17	0.247
33	0.246
45	0.248
60	0.251

2.3. Training and Testing of the ANN-Based Model

For verification and checkup of the prediction capability of the ANN-based model, the gathered data were separated to 2 parts: 70% of the data for the training subset and 30% for the testing subset. The TRIANBR function, as the fastest backpropagation algorithm, was employed for the training part that updates the weight and bias values based on Bayesian regularization optimization. In addition, for minimization of errors, the function of gradient descent with momentum weight and bias learning (LEARNGDM) was applied. LEARNGDM estimates the weight change for a specific neuron from the neuron's input and error, the weight/bias, learning rate and momentum constant, relying on the gradient descent along with momentum backpropagation. The considered subsets for training and testing of the model were chosen randomly from the available database. Furthermore, a hyperbolic tangent sigmoid was used as an activation function in the hidden layer and for this task in the output layer, linear functions were employed. The performance of these functions has been proved in other research works [39,42,44,45,89–93].

In order to assess the prediction capability of the ANN-based model, two indexes of root mean square error (RMSE) and absolute fraction of variance (R^2) were used. The RMSE and R^2 can be calculated by using Equations (2) and (3) [44].

$$RMSE = \left((\frac{1}{p}) \sum_j \left| T_j - O_j \right|^2 \right)^{\frac{1}{2}} \quad (2)$$

$$R^2 = 1 - \left(\frac{\sum_j (T_j - O_j)^2}{\sum_j (O_j)^2} \right) \quad (3)$$

where, p represents the number of cases, T_j is the target value (i.e., simulation results) and O_j is the output value (i.e., model predictions).

2.4. Calculation of Relative Impact of Inputs on the Output

To estimate the influences of input variables on the output, the indicator of relative impact was applied. In this study, the effect of input variables on the output was analyzed by using the equation of Garson that is based on the matrix of the neural net weight [88]. In the Garson equation, the numerator is determined by the summation of the absolute weight of products for any input and the denominator is defined by summation of all weights feeding into the hidden unit. The fitting Garson equation for the current ANN topology is shown in Equation (4).

$$I_i = \frac{\sum_{j=1}^{j=13}\left(\left(\frac{\left|IW_{j,i}\right|}{\sum_{i=1}^{i=12}\left|IW_{j,i}\right|}\right).\left|LW_{j,i}\right|\right)}{\sum_{i=1}^{i=12}\left\{\sum_{j=1}^{j=13}\left(\left(\frac{\left|IW_{j,i}\right|}{\sum_{i=1}^{i=12}\left|IW_{j,i}\right|}\right).\left|LW_{j,i}\right|\right)\right\}} \quad (4)$$

In Equation (4), i represents the input variables, j is used for the neurons in the hidden layer, I_i represents the relative impact of the ith input variable on the output, $IW_{j,i}$ serves as the weight of the ith neuron of hidden layer from the ith input variable, $LW_{j,i}$ shows the weight to the output layer from the ith neuron of the hidden layer and the number of neurons is shown by n (13 for $\mathrm{sm}_{\mathrm{hydrogen}}$). Afterwards, for calculation of the relative impact of the inputs on the output, the input variables were ranked and compared.

3. Results and Discussion

The developed ANN-based model, by considering 12 inputs, one output and 13 neurons in the hidden layer, was recognized as a proper and efficient way in prediction of the specific flow rate of hydrogen. The ANN models were primarily based on weights and biases (shown as IW and b in Figure 2) that are the learnable parameters of a machine learning model. In fact, the weights and biases are possibly the most important concepts of a neural network. When the inputs are transmitted between neurons, the weights are applied to the inputs and passed into an activation function along with the bias.

Weights control the signal or the strength of the connection between two neurons. In other words, a weight decides how much influence the input will have on the output.

Biases, which are constant, are an additional input into the next layer and they are not influenced by the previous layer. They do not have any incoming connections but they have outgoing connections with their own weights. The bias unit guarantees that even when all the inputs are zeros, there will still be an activation in the neuron.

The best fitting values for parameters of $IW_{j,i}$, $LW_{1,j}$, b_{1j}, b_2 at 13 neurons in the hidden layer of the ANN-based model implemented for the downdraft biomass gasification model are depicted in Tables 3 and 4.

Table 3. The weights of inputs to the ANN model for prediction of $sm_{hydrogen}$.

Neuron	M [%]	VM [%]	FC [%]	A [%]	C [%]	O [%]	H [%]	N [%]	S [%]	T [°C]	ARF	SBR
1	−0.01	−0.09	−0.05	−0.12	−0.03	−0.04	−0.22	0.02	0.04	0.05	−0.01	−0.46
2	−0.64	0.06	0.01	0.34	−0.30	0.48	−0.32	0.11	0.12	−0.02	0.17	−0.10
3	0.13	−0.06	−0.03	0.02	−0.13	0.10	−0.19	0.01	0.03	0.52	0.08	−0.04
4	−0.13	0.33	0.23	0.31	0.61	−0.14	0.09	0.04	−0.05	−1.57	−0.21	−1.05
5	−0.07	0.13	0.08	0.17	0.16	−0.02	0.15	0.00	0.01	2.43	−0.06	0.00
6	0.03	−0.09	−0.06	0.07	−0.41	0.28	0.02	0.02	0.03	−0.03	0.14	1.24
7	0.14	0.1	0.06	−0.00	0.35	−0.21	−0.01	−0.02	−0.03	−0.12	−0.11	−0.9
8	−0.07	0.09	0.05	0.09	0.13	−0.05	0.14	0.00	0.00	1.45	−0.05	0.01
9	−0.23	0.12	0.07	0.15	0.09	0.03	0.21	−0.01	−0.03	0.04	−0.01	0.33
10	0.17	0.11	0.06	0.08	0.27	−0.11	−0.02	−0.03	−0.03	0.42	−0.06	−0.88
11	−2.92	0.50	0.15	0.80	0.66	0.28	−1.06	0.21	0.57	0.01	0.04	0.08
12	2.45	−0.49	−0.18	−0.81	−0.60	−0.28	0.84	−0.17	−0.44	−0.01	−0.03	−0.06
13	0.12	0.06	0.03	−0.00	0.17	−0.08	−0.01	−0.01	0.02	−0.11	1.49	−0.37

Table 4. The biases (b_{1j}, b_0) and weights ($LW_{1,j}$) of hidden layer to output layer for the case of $sm_{hydrogen}(kg/kg)$.

	Neuron	Weights to Output Layer	Bias
Hidden Layer	1	1.1628	0.5408
	2	−0.1604	−0.8705
	3	−0.6471	0.1494
	4	−0.1117	−1.7707
	5	−0.9983	−0.7854
	6	−0.7558	0.1433
	7	−0.9249	−0.3068
	8	1.3991	−0.4846
	9	1.7991	−0.7057
	10	−0.2568	−0.5060
	11	0.8289	−3.1088
	12	1.9675	3.1332
	13	0.0355	−0.1756
Output Layer	1	-	−1.1572

The extracted data from the simulation and prediction of $sm_{hydrogen}$ were compared adequately and competently by applying linear regression approaches in the ANN-based model for training and testing subsets. Figure 3 shows the targets for training, testing and all targets together. Obviously, for all sets, the R^2 value is higher than 0.999 and the RMSE value is lower than 0.25 for $sm_{hydrogen}$ as a product of the gasification system connected with a hydrogen plant. Furthermore, for more assurance, the forecasted and simulated output data of $sm_{hydrogen}$ for several cases are depicted in Figure 4. The satisfactory comparison of these types of data and only a slight deviation in Figure 4 prove that the developed ANN model is assuredly sound and acceptable.

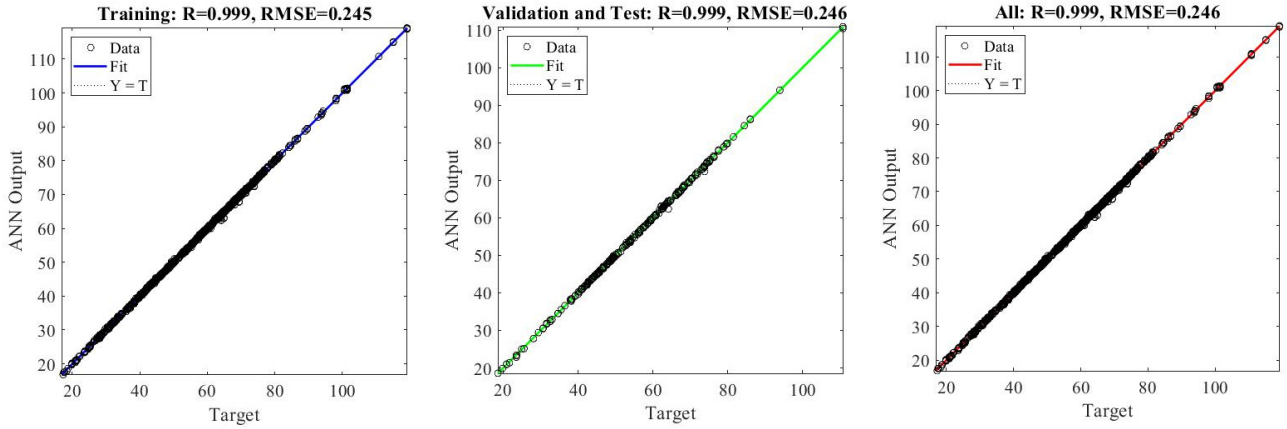

Figure 3. Comparing of simulation and prediction of $sm_{hydrogen}$ for training, testing and all targets together.

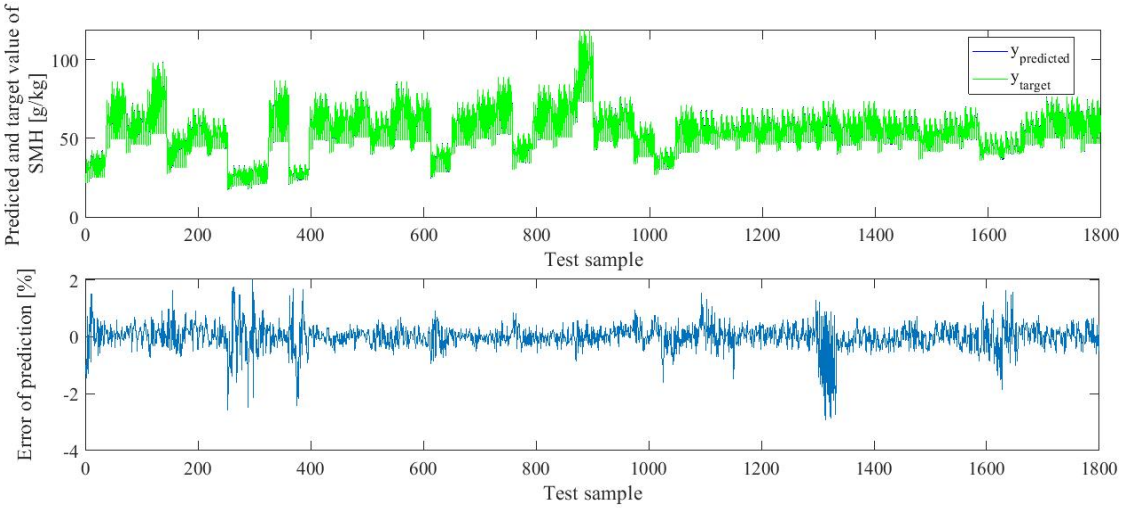

Figure 4. Comparison of the predicted and simulated output data of $sm_{hydrogen}$ for several cases.

As it mentioned in the methodology section, the equation of Garson was applied to evaluate the effects of the 12 inputs on the output. The relative impact of inputs on the $sm_{hydrogen}$ as output of the system is shown in Figure 5. It is observed that the most effective parameters are gasifier temperature, SBR, moisture content and hydrogen, with contributions of 19.96, 17.18, 15.3 and 10.48%, respectively. In fact, temperature growth presents greater benefits for the creation of H_2 and CO, which produce a large amount of gas (syngas) and, consequently, hydrogen in the output of the system. The other variables of feed properties like C, O, S and N contribute in the range of 1.28–8.6% and proximate components like VM, FC and A contribute in the range of 3.14–7.67% to the impact on $sm_{hydrogen}$. Obviously, the mass flow rate of air to fuel ratio (AFR) with a share of 2.4% is at the bottom of variable list in view of the impact on $sm_{hydrogen}$. This means that the variation in the air flow rate entering the gasifier has a negligible impact on the hydrogen production and the AFR can be in the window of 1.8–2.3 for woody, herbaceous and agricultural biomasses, and there is no need to fix a point.

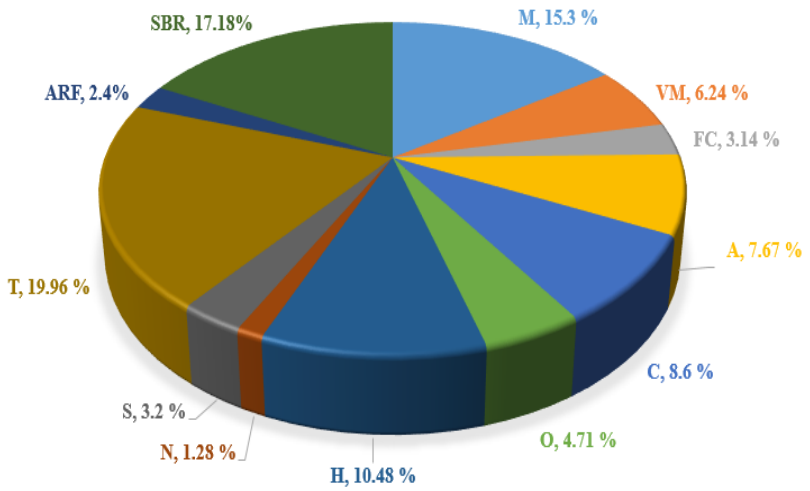

Figure 5. Relative impact (%) of inputs on $sm_{hydrogen}$.

A sensitivity assessment was performed to carry out an extra broad evaluation. The alterations of the inputs corresponding to hydrogen content are shown by eleven plots

with three-dimensional contours in Figure 6. SMH in Figure 6 is an abbreviation of the specific mass flow rate of hydrogen. It can be observed that by increasing the hydrogen content and temperature/SBR/carbon content/VM in feeds, a greater quantity of biohydrogen is obtained through the gasifier. Nevertheless, 900–1100 °C is the optimum range of the gasifier temperature, which led to the highest production of hydrogen from the feedstocks. Moisture content and oxygen show the opposite trend where, by decreasing them and increasing the hydrogen content, the production of hydrogen is increased. It can also be seen that high levels of hydrogen, nitrogen and sulfur content in the studied biomasses have neutral effects on the output. Overall, the optimal compositions and conditions to obtain optimal production of biohydrogen are shown in Table 5.

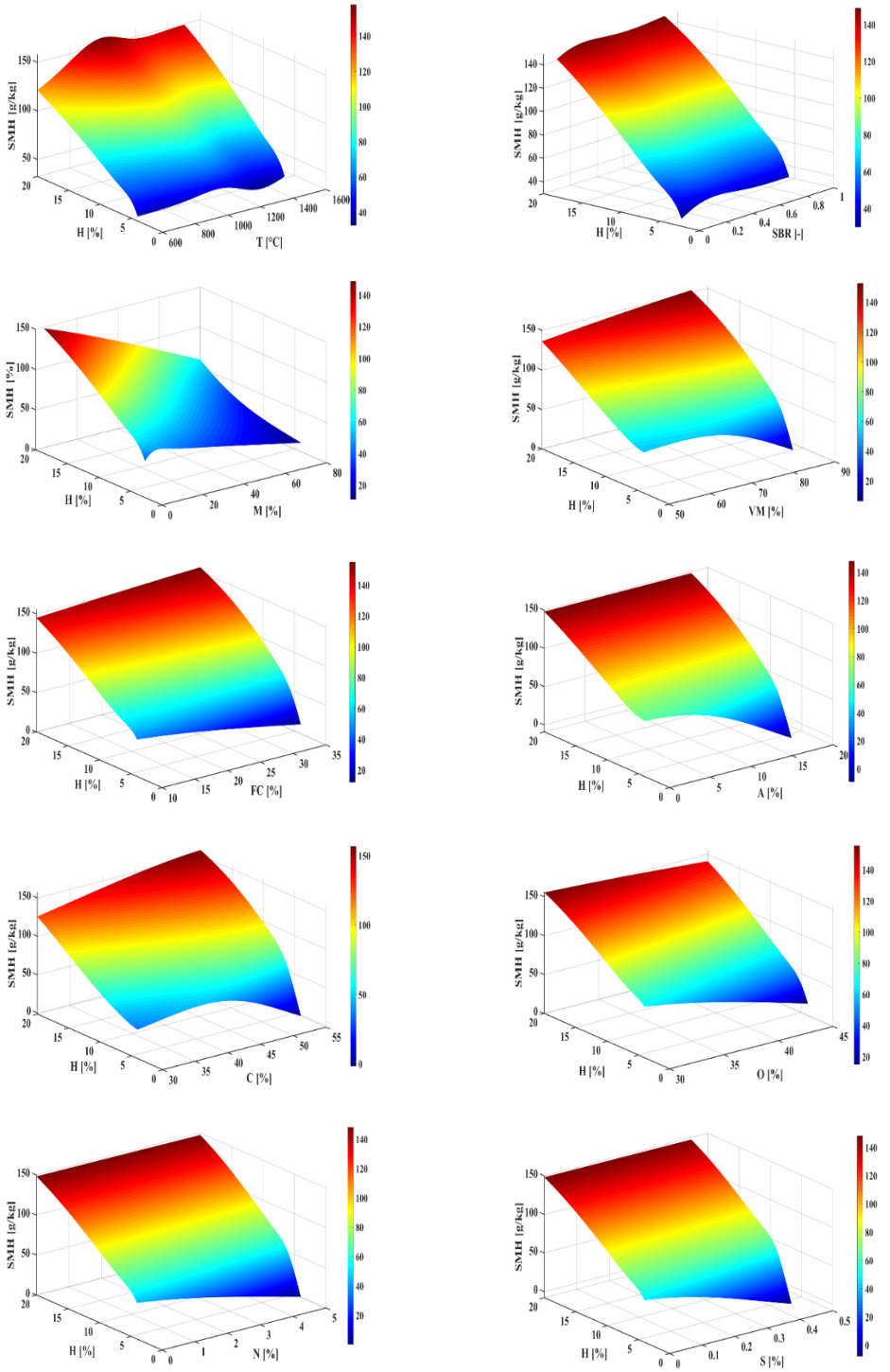

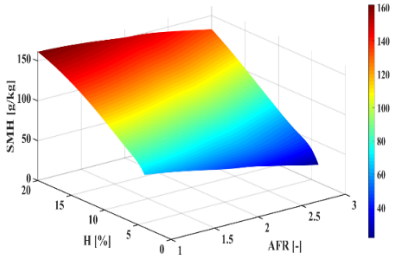

Figure 6. Sensitivity assessments plots (SMH is abbreviation of specific mass flow rate of hydrogen).

Table 5. The optimal compositions and conditions for optimal production of biohydrogen.

Inputs	H_2	C	O	N&S	M	VM	FC	Ash	SBR	T	AFR
Optimal Range	17–20	45–55	30–35	<1	<5	64–86	12–26	<15	0.7–0.8	900–1100	1.8–2.3

4. Conclusions

Broadly speaking, only a few studies have reported about biomass gasification modeling according to an ANN-based approach and there is nothing on gasification integrated with a water–gas shift unit and separation unit for hydrogen production. Therefore, we attempted to firstly develop an ANN-based model to anticipate the specific mass flow rate of hydrogen from gasification connected with a hydrogen plant.

The established ANN-based model in this work indicates satisfactory and sound results with an R^2 value of more than 0.999 and an RMSE value lower than 0.25 for $sm_{hydrogen}$ as a product from a gasification system connected with a hydrogen plant. Almost all of the inputs show a significant impact on the $sm_{hydrogen}$ output. Significantly, gasifier temperature, SBR, moisture content and hydrogen have the highest impacts on the $sm_{hydrogen}$ with contributions of 19.96, 17.18, 15.3 and 10.48%, respectively. In addition, other variables of feed properties like C, O, S and N contribute in the range of 1.28–8.6% and proximate components like VM, FC and A contribute in the range of 3.14–7.67% to the impact on $sm_{hydrogen}$.

The accurate results obtained for the biohydrogen production via the gasification system connected with water–gas shift reactors confirms the strong prediction ability of the developed ANN-based model with one hidden layer with 13 neurons, through applying a backpropagation algorithm. The developed model has the capability to be employed with a broad range of biomasses. In addition, the results illustrate the relative impact of various biomass properties and operating parameters on the biohydrogen output from the system. The developed model can be used practically for the screening of suitable biomasses for hydrogen extraction based on a gasification system connected with W–G shift and a hydrogen recovery unit.

Author Contributions: S.S.: Conceptualization, Methodology, Validation, Formal analysis, Investigation, Resources, Writing—original draft. S.M.E.S.: Conceptualization, Methodology, Validation, Formal analysis, Investigation. R.U.: Supervision. C.R.: Software, Supervision. All authors have read and agreed to the published version of the manuscript.

Funding: This paper was a part of the project funded by Icelandic Research Fund (IRF), (in Icelandic: Rannsoknasjodur) and the grant number is 196458-051.

Institutional Review Board Statement: Not applicable.

Informed Consent Statement: Not applicable.

Data Availability Statement: Not applicable.

Conflicts of Interest: The authors declare no conflict of interest.

References

1. Safarian, S.; Khodaparast, P.; Kateb, M. Modeling and technical-economic optimization of electricity supply network by three photovoltaic systems. *J. Sol. Energy Eng.* **2014**, *136*, 024501.
2. Rajaeifar, M.A.; Akram, A.; Ghobadian, B.; Rafiee, S.; Heijungs, R.; Tabatabaei, M. Environmental impact assessment of olive pomace oil biodiesel production and consumption: A comparative lifecycle assessment. *Energy* **2016**, *106*, 87–102.
3. Talebnia, F.; Karakashev, D.; Angelidaki, I. Production of bioethanol from wheat straw: An overview on pretreatment, hydrolysis and fermentation. *Bioresour. Technol.* **2010**, *101*, 4744–4753.
4. Safarian, S.; Unnthorsson, R.; Richter, C. Techno-economic analysis of power production by using waste biomass gasification. *J. Power Energy Eng.* **2020**, *8*, 1–8.
5. Zeng, J.; Xiao, R.; Zhang, H.; Wang, Y.; Zeng, D.; Ma, Z. Chemical looping pyrolysis-gasification of biomass for high h2/co syngas production. *Fuel Process. Technol.* **2017**, *168*, 116–122.
6. Luo, H.; Lin, W.; Song, W.; Li, S.; Dam-Johansen, K.; Wu, H. Three dimensional full-loop cfd simulation of hydrodynamics in a pilot-scale dual fluidized bed system for biomass gasification. *Fuel Process. Technol.* **2019**, *195*, 106146.
7. Kumar, B.; Bhardwaj, N.; Agrawal, K.; Chaturvedi, V.; Verma, P. Current perspective on pretreatment technologies using lignocellulosic biomass: An emerging biorefinery concept. *Fuel Process. Technol.* **2020**, *199*, 106244.
8. Safarian, S.; Sattari, S.; Hamidzadeh, Z. Sustainability assessment of biodiesel supply chain from various biomasses and conversion technologies. *Biophys. Econ. Resour. Qual.* **2018**, *3*, 6.
9. Safarian, S.; Sattari, S.; Unnthorsson, R.; Hamidzadeh, Z. Prioritization of bioethanol production systems from agricultural and waste agricultural biomass using multi-criteria decision making. *Biophys. Econ. Resour. Qual.* **2019**, *4*, 4.
10. Safarian, S.; Unnthorsson, R. An assessment of the sustainability of lignocellulosic bioethanol production from wastes in iceland. *Energies* **2018**, *11*, 1493.
11. Nguyen, T.L.T.; Hermansen, J.E.; Nielsen, R.G. Environmental assessment of gasification technology for biomass conversion to energy in comparison with other alternatives: The case of wheat straw. *J. Clean. Prod.* **2013**, *53*, 138–148.
12. Huda, A.; Mekhilef, S.; Ahsan, A. Biomass energy in bangladesh: Current status and prospects. *Renew. Sustain. Energy Rev.* **2014**, *30*, 504–517.
13. Safarian, S.; Unnþórsson, R.; Richter, C. A review of biomass gasification modelling. *Renew. Sustain. Energy Rev.* **2019**, *110*, 378–391.
14. Inayat, A.; Raza, M.; Khan, Z.; Ghenai, C.; Aslam, M.; Shahbaz, M.; Ayoub, M. Flowsheet modeling and simulation of biomass steam gasification for hydrogen production. *Chem. Eng. Technol.* **2020**, *43*, 649–660.
15. Safarian, S.; Saryazdi, S.M.E.; Unnthorsson, R.; Richter, C. Artificial neural network integrated with thermodynamic equilibrium modeling of downdraft biomass gasification-power production plant. *Energy* **2020**, *213*, 118800.
16. Safarian, S.; Unnthorsson, R.; Richter, C. The equivalence of stoichiometric and non-stoichiometric methods for modeling gasification and other reaction equilibria. *Renew. Sustain. Energy Rev.* **2020**, *131*, 109982.
17. All Power Laboratories. Available online: http://www.allpowerlabs.com/ (accessed on 12 Dec 2019).
18. Safarian, S.; Unnthorsson, R.; Richter, C. Simulation and performance analysis of integrated gasification–syngas fermentation plant for lignocellulosic ethanol production. *Fermentation* **2020**, *6*, 68.
19. Marcantonio, V.; De Falco, M.; Capocelli, M.; Bocci, E.; Colantoni, A.; Villarini, M. Process analysis of hydrogen production from biomass gasification in fluidized bed reactor with different separation systems. *Int. J. Hydrog. Energy* **2019**, *44*, 10350–10360.
20. Safarian, S.; Unnthorsson, R.; Richter, C. Gasification of Woody Biomasses and Forestry Residues: Simulation, Performance Analysis, and Environmental Impact *Energy* **2020**, *197*, 117268.
21. Balat, H.; Kırtay, E. Hydrogen from biomass–present scenario and future prospects. *Int. J. Hydrog. Energy* **2010**, *35*, 7416–7426.
22. Martin, M.; Svensson, N.; Fonseca, J.; Eklund, M. Quantifying the environmental performance of integrated bioethanol and biogas production. *Renew. Energy* **2014**, *61*, 109–116.
23. Yoon, S.J.; Son, Y.-I.; Kim, Y.-K.; Lee, J.-G. Gasification and power generation characteristics of rice husk and rice husk pellet using a downdraft fixed-bed gasifier. *Renew. Energy* **2012**, *42*, 163–167.

24. Safarian, S.; Saboohi, Y.; Kateb, M. Evaluation of energy recovery and potential of hydrogen production in iranian natural gas transmission network. *Energy Policy* **2013**, *61*, 65–77.
25. Çağlar, A.; Demirbaş, A. Hydrogen rich gas mixture from olive husk via pyrolysis. *Energy Convers. Manag.* **2002**, *43*, 109–117.
26. Frigo, S.; Spazzafumo, G. Cogeneration of power and substitute of natural gas using biomass and electrolytic hydrogen. *Int. J. Hydrog. Energy* **2018**, *43*, 11696–11705.
27. Li, Q.; Song, G.; Xiao, J.; Sun, T.; Yang, K. Exergy analysis of biomass staged-gasification for hydrogen-rich syngas. *Int. J. Hydrog. Energy* **2019**, *44*, 2569–2579.
28. Safarian, S.; Richter, C.; Unnthorsson, R. Waste biomass gasification simulation using aspen plus: Performance evaluation of wood chips, sawdust and mixed paper wastes. *J. Power Energy Eng.* **2019**, *7*, 12–30.
29. S S, Safarian; S.M. Ebrahimi, Saryazdi; R. Unnthorsson; C, Richter. Performance analysis and environmental assessment of small-scale waste biomass gasification integrated chp in iceland. *Fermentation* **2020**, *7*, 61.
30. Safarian, S.; Unnthorsson, R.; Richter, C. Simulation of small-scale waste biomass gasification integrated power production: A comparative performance analysis for timber and wood waste. *Int. J. Appl. Power Eng. IJAPE* **2020**, *9*, 147–152.
31. Safarian, S.; Unnthorsson, R.; Richter, C. Techno-economic and environmental assessment of power supply chain by using waste biomass gasification in iceland. *Biophys. Econ. Sustain.* **2020**, *5*, 7.
32. Damartzis, T.; Michailos, S.; Zabaniotou, A. Energetic assessment of a combined heat and power integrated biomass gasification–internal combustion engine system by using aspen plus®. *Fuel Process. Technol.* **2012**, *95*, 37–44.
33. Kobayashi, N.; Tanaka, M.; Piao, G.; Kobayashi, J.; Hatano, S.; Itaya, Y.; Mori, S. High temperature air-blown woody biomass gasification model for the estimation of an entrained down-flow gasifier. *Waste Manag.* **2009**, *29*, 245–251.
34. Porcu, A.; Sollai, S.; Marotto, D.; Mureddu, M.; Ferrara, F.; Pettinau, A. Techno-economic analysis of a small-scale biomass-to-energy bfb gasification-based system. *Energies* **2019**, *12*, 494.
35. Roy, D.; Samanta, S.; Ghosh, S. Thermo-economic assessment of biomass gasification-based power generation system consists of solid oxide fuel cell, supercritical carbon dioxide cycle and indirectly heated air turbine. *Clean Technol. Environ. Policy* **2019**, *21*, 827–845.
36. Safarianbana, S.; Unnthorsson, R.; Richter, C. Development of a new stoichiometric equilibrium-based model for wood chips and mixed paper wastes gasification by aspen plus. In *ASME International Mechanical Engineering Congress and Exposition*; American Society of Mechanical Engineers, Salt Lake City, Utah, USA. 2019; p. V006T006A002.
37. Shayan, E.; Zare, V.; Mirzaee, I. Hydrogen production from biomass gasification; a theoretical comparison of using different gasification agents. *Energy Convers. Manag.* **2018**, *159*, 30–41.
38. Gil, J.; Corella, J.; Aznar, M.A.P.; Caballero, M.A. Biomass gasification in atmospheric and bubbling fluidized bed: Effect of the type of gasifying agent on the product distribution. *Biomass Bioenergy* **1999**, *17*, 389–403.
39. George, J.; Arun, P.; Muraleedharan, C. Assessment of producer gas composition in air gasification of biomass using artificial neural network model. *Int. J. Hydrog. Energy* **2018**, *43*, 9558–9568.
40. Nasir, V.; Nourian, S.; Avramidis, S.; Cool, J. Classification of thermally treated wood using machine learning techniques. *Wood Sci. Technol.* **2019**, *53*, 275–288.
41. Nasir, V.; Nourian, S.; Avramidis, S.; Cool, J. Prediction of physical and mechanical properties of thermally modified wood based on color change evaluated by means of "group method of data handling" (gmdh) neural network. *Holzforschung* **2019**, *73*, 381–392.
42. Rostampour, V.; Motlagh, A.M.; Komarizadeh, M.H.; Sadeghi, M.; Bernousi, I.; Ghanbari, T. Using artificial neural network (ann) technique for prediction of apple bruise damage. *Aust. J. Crop Sci.* **2013**, *7*, 1442–1448.
43. Capizzi, G.; Sciuto, G.L.; Napoli, C.; Woźniak, M.; Susi, G. A spiking neural network-based long-term prediction system for biogas production. *Neural Netw.* **2020**, *129*, 271–279.
44. Baruah, D.; Baruah, D.; Hazarika, M. Artificial neural network based modeling of biomass gasification in fixed bed downdraft gasifiers. *Biomass Bioenergy* **2017**, *98*, 264–271.
45. Puig-Arnavat, M.; Hernández, J.A.; Bruno, J.C.; Coronas, A. Artificial neural network models for biomass gasification in fluidized bed gasifiers. *Biomass Bioenergy* **2013**, *49*, 279–289.
46. Schmidt, A.; Creason, W.; Law, B.E. Estimating regional effects of climate change and altered land use on biosphere carbon fluxes using distributed time delay neural networks with bayesian regularized learning. *Neural Netw.* **2018**, *108*, 97–113.
47. Safarian, S.; Saryazdi, S.M.E.; Unnthorsson, R.; Richter, C. Artificial neural network modeling of bioethanol production via syngas fermentation. *Biophys. Econ. Sustain.* **2021**, *6*, 1–13.
48. Safarian, S.; Bararzadeh, M. Exergy analysis of high-performance cycles for gas turbine with air-bottoming. *J. Mech. Eng. Res.* **2012**, *5*, 38–49.
49. Safarian, S.; Unnthorsson, R.; Richter, C. Performance analysis of power generation by wood and woody biomass gasification in a downdraft gasifier. *J. Appl. Power Eng.* **2021**, *10*, 80–88.
50. Vassilev, S.V.; Baxter, D.; Andersen, L.K.; Vassileva, C.G. An overview of the chemical composition of biomass. *Fuel* **2010**, *89*, 913–933.
51. Miles, T.; Baxter, L.; Bryers, R.; Jenkins, B.; Oden, L. Alkali deposits found in biomass power plants: A preliminary investigation of their extent and nature. **1995**, doi:10.2172/251288.
52. Bryers, R.W. Fireside slagging, fouling, and high-temperature corrosion of heat-transfer surface due to impurities in steam-raising fuels. *Prog. Energy Combust. Sci.* **1996**, *22*, 29–120.

53. Theis, M.; Skrifvars, B.-J.; Hupa, M.; Tran, H. Fouling tendency of ash resulting from burning mixtures of biofuels. Part 1: Deposition rates. *Fuel* **2006**, *85*, 1125–1130.
54. Theis, M.; Skrifvars, B.-J.; Zevenhoven, M.; Hupa, M.; Tran, H. Fouling tendency of ash resulting from burning mixtures of biofuels. Part 2: Deposit chemistry. *Fuel* **2006**, *85*, 1992–2001.
55. Zevenhoven-Onderwater, M.; Backman, R.; Skrifvars, B.-J.; Hupa, M. The ash chemistry in fluidised bed gasification of biomass fuels. Part i: Predicting the chemistry of melting ashes and ash–bed material interaction. *Fuel* **2001**, *80*, 1489–1502.
56. Zevenhoven-Onderwater, M.; Blomquist, J.-P.; Skrifvars, B.-J.; Backman, R.; Hupa, M. The prediction of behaviour of ashes from five different solid fuels in fluidised bed combustion. *Fuel* **2000**, *79*, 1353–1361.
57. Demirbas, A. Combustion characteristics of different biomass fuels. *Prog. Energy Combust. Sci.* **2004**, *30*, 219–230.
58. Vamvuka, D.; Zografos, D. Predicting the behaviour of ash from agricultural wastes during combustion. *Fuel* **2004**, *83*, 2051–2057.
59. Vamvuka, D.; Zografos, D.; Alevizos, G. Control methods for mitigating biomass ash-related problems in fluidized beds. *Bioresour. Technol.* **2008**, *99*, 3534–3544.
60. Moilanen, A. *Thermogravimetric Characterisations of Biomass and Waste for Gasification Processes*; VTT: 2006. https://www.vttresearch.com/sites/default/files/pdf/publications/2006/P607.pdf
61. Masiá, A.T.; Buhre, B.; Gupta, R.; Wall, T. Characterising ash of biomass and waste. *Fuel Process. Technol.* **2007**, *88*, 1071–1081.
62. Lapuerta, M.; Hernández, J.J.; Pazo, A.; López, J. Gasification and co-gasification of biomass wastes: Effect of the biomass origin and the gasifier operating conditions. *Fuel Process. Technol.* **2008**, *89*, 828–837.
63. Tillman, D.A. Biomass cofiring: The technology, the experience, the combustion consequences. *Biomass Bioenergy* **2000**, *19*, 365–384.
64. Demirbas, A. Potential applications of renewable energy sources, biomass combustion problems in boiler power systems and combustion related environmental issues. *Prog. Energy Combust. Sci.* **2005**, *31*, 171–192.
65. Wei, X.; Schnell, U.; Hein, K.R. Behaviour of gaseous chlorine and alkali metals during biomass thermal utilisation. *Fuel* **2005**, *84*, 841–848.
66. Scurlock, J.M.; Dayton, D.C.; Hames, B. Bamboo: An overlooked biomass resource? *Biomass Bioenergy* **2000**, *19*, 229–244.
67. Risnes, H.; Fjellerup, J.; Henriksen, U.; Moilanen, A.; Norby, P.; Papadakis, K.; Posselt, D.; Sørensen, L. Calcium addition in straw gasification☆. *Fuel* **2003**, *82*, 641–651.
68. Thy, P.; Jenkins, B.; Grundvig, S.; Shiraki, R.; Lesher, C. High temperature elemental losses and mineralogical changes in common biomass ashes. *Fuel* **2006**, *85*, 783–795.
69. Thy, P.; Lesher, C.; Jenkins, B. Experimental determination of high-temperature elemental losses from biomass slag. *Fuel* **2000**, *79*, 693–700.
70. Wieck-Hansen, K.; Overgaard, P.; Larsen, O.H. Cofiring coal and straw in a 150 mwe power boiler experiences. *Biomass Bioenergy* **2000**, *19*, 395–409.
71. Nutalapati, D.; Gupta, R.; Moghtaderi, B.; Wall, T. Assessing slagging and fouling during biomass combustion: A thermodynamic approach allowing for alkali/ash reactions. *Fuel Process. Technol.* **2007**, *88*, 1044–1052.
72. Werther, J.; Saenger, M.; Hartge, E.-U.; Ogada, T.; Siagi, Z. Combustion of agricultural residues. *Prog. Energy Combust. Sci.* **2000**, *26*, 1–27.
73. Srikanth, S.; Das, S.K.; Ravikumar, B.; Rao, D.; Nandakumar, K.; Vijayan, P. Nature of fireside deposits in a bagasse and groundnut shell fired 20 mw thermal boiler. *Biomass Bioenergy* **2004**, *27*, 375–384.
74. Madhiyanon, T.; Sathitruangsak, P.; Soponronnarit, S. Co-combustion of rice husk with coal in a cyclonic fluidized-bed combustor (ψ-fbc). *Fuel* **2009**, *88*, 132–138.
75. Pettersson, A.; Zevenhoven, M.; Steenari, B.-M.; Åmand, L.-E. Application of chemical fractionation methods for characterisation of biofuels, waste derived fuels and cfb co-combustion fly ashes. *Fuel* **2008**, *87*, 3183–3193.
76. Tite, M.S.; Shortland, A.; Maniatis, Y.; Kavoussanaki, D.; Harris, S. The composition of the soda-rich and mixed alkali plant ashes used in the production of glass. *J. Archaeol. Sci.* **2006**, *33*, 1284–1292.
77. Ross, A.; Jones, J.; Kubacki, M.; Bridgeman, T. Classification of macroalgae as fuel and its thermochemical behaviour. *Bioresour. Technol.* **2008**, *99*, 6494–6504.
78. Vassilev, S.V.; Vassileva, C.G. A new approach for the combined chemical and mineral classification of the inorganic matter in coal. 1. Chemical and mineral classification systems. *Fuel* **2009**, *88*, 235–245.
79. Safarian, S.; Saryazdi, S.M.E.; Unnthorsson, R.; Richter, C. Dataset of biomass characteristics and net output power from downdraft biomass gasifier integrated power production unit. *Data Brief* **2020**, *33*, 106390.
80. Tauqir, W.; Zubair, M.; Nazir, H. Parametric analysis of a steady state equilibrium-based biomass gasification model for syngas and biochar production and heat generation. *Energy Convers. Manag.* **2019**, *199*, 111954.
81. Preciado, J.E.; Ortiz-Martinez, J.J.; Gonzalez-Rivera, J.C.; Sierra-Ramirez, R.; Gordillo, G. Simulation of synthesis gas production from steam oxygen gasification of colombian coal using aspen plus®. *Energies* **2012**, *5*, 4924–4940.
82. Sjardin, M.; Damen, K.; Faaij, A. Techno-economic prospects of small-scale membrane reactors in a future hydrogen-fuelled transportation sector. *Energy* **2006**, *31*, 2523–2555.
83. Li, A.; Liang, W.; Hughes, R. The effect of carbon monoxide and steam on the hydrogen permeability of a pd/stainless steel membrane. *J. Membr. Sci.* **2000**, *165*, 135–141.

84. Carrara, A.; Perdichizzi, A.; Barigozzi, G. Simulation of an hydrogen production steam reforming industrial plant for energetic performance prediction. *Int. J. Hydrog. Energy* **2010**, *35*, 3499–3508.
85. Sircar, S.; Waldron, W.E.; Anand, M.; Rao, M.B. Hydrogen Recovery by Pressure Swing Adsorption Integrated with Adsorbent Membranes. U.S. Patent 5753010, 19 May 1998.
86. Pallozzi, V.; Di Carlo, A.; Bocci, E.; Villarini, M.; Foscolo, P.; Carlini, M. Performance evaluation at different process parameters of an innovative prototype of biomass gasification system aimed to hydrogen production. *Energy Convers. Manag.* **2016**, *130*, 34–43.
87. Honeywell, Uop. Years of psa technology for h2 purification. **2016**. https://uop.honeywell.com/en/industry-solutions/refining/hydrogen-recovery/polybed-psa-systems (accessed on 21 Jan 2021)
88. Antonopoulos, I.-S.; Karagiannidis, A.; Gkouletsos, A.; Perkoulidis, G. Modelling of a downdraft gasifier fed by agricultural residues. *Waste Manag.* **2012**, *32*, 710–718.
89. Elmaz, F.; Yücel, Ö.; Mutlu, A.Y. Predictive modeling of biomass gasification with machine learning-based regression methods. *Energy* **2020**, *191*, 116541.
90. Li, H.; Xu, Q.; Xiao, K.; Yang, J.; Liang, S.; Hu, J.; Hou, H.; Liu, B. Predicting the higher heating value of syngas pyrolyzed from sewage sludge using an artificial neural network. *Environ. Sci. Pollut. Res.* **2020**, *27*, 785–797.
91. Neill, S.P.; Hashemi, M.R. *Fundamentals of Ocean Renewable Energy: Generating Electricity from the Sea*; Academic Press, Elsevier: 2018.
92. Serrano, D.; Golpour, I.; Sánchez-Delgado, S. Predicting the effect of bed materials in bubbling fluidized bed gasification using artificial neural networks (anns) modeling approach. *Fuel* **2020**, *266*, 117021.
93. Pandey, D.S.; Das, S.; Pan, I.; Leahy, J.J.; Kwapinski, W. Artificial neural network based modelling approach for municipal solid waste gasification in a fluidized bed reactor. *Waste Manag.* **2016**, *58*, 202–213.